Algorithmic Description of Hippocampal Granule Cell Dendritic Morphology

Alexei V. Samsonovich[1], Giorgio A. Ascoli[2*]

[1]*Krasnow Institute for Advanced Study, George Mason University, Fairfax, VA 22030-4444.*

[2]*Krasnow Institute for Advanced Study and Psychology Department, George Mason University, Fairfax, VA 22030-4444.*

Abstract

Recent efforts in computational neuroanatomy have aimed at accurately reproducing all relevant statistical details of dendritic morphology with stochastic models based on local rules and parameters measured from real neurons. Here we present a solution of this problem for dentate gyrus granule cells based on a hidden Markov algorithm. The correctness of the model is supported by the statistical agreement between distributions of emergent parameters measured from population of traced and virtual neurons. The algorithm relies on two local hidden variables, one of which might be associated with dendritic microtubules, and another may represent the time of development.

Keywords: 3D model; Dentate Gyrus; Granule Cell; Hidden Markov; Morphometry.

* Corresponding author.
E-mail address: ascoli@gmu.edu (G.A. Ascoli).

1. Introduction

An intriguing question in hippocampal cellular neuroanatomy research is whether or not the dendritic morphology of principal cells can be captured by a concise, local-rule-based statistical model that allows for its implementation as a simple computational algorithm [1-2]. The present work gives a positive answer to this problem. More precisely, here the dendritic morphology of the rat dentate gyrus granule cells is described accurately in all its functionally relevant statistical details by an elegant hidden-Markov (i.e., feed-forward, local and causal) algorithm. In addition, the hidden variables of the algorithm allow for plausible biophysical interpretations.

2. Materials and Methods

Digital data of reconstructed rat dentate gyrus granule cells [3-4] were kindly made available by Dr. B. J. Claiborne (University of Texas at San Antonio) through the Internet (www.utsa.edu/claibornelab). In these data files, neurons are represented as binary tree structures constructed with a finite set of cylindrical segments, each with an individual parent in the path to the root (soma), and with 0, 1, or 2 "daughter" segments at the opposite end (constituting termination, continuation, or bifurcation points). Here a *branch* is defined as a segment or a chain of segments connected by continuation points, that does not start or end with a continuation point. Only 36 of the 42 cells in this archive were used for quantitative analysis: in 6 cases minor inconsistencies in the data files prevented numerical processing (cells 1208875, 3319201, 411883, 411884A, 411884B, 803887B). Dendrites of the remaining 36 cells had 512(±188) continuation points and 14(±3) bifurcations per cell.

Parts of the model used in this work were previously described [5-8]. In essence, the algorithm is divided in three phases. Phase 1 consists of the "virtual growth" of a skeletonized dendrogram (i.e., a dendrogram without the diameter information) starting from the soma and dendritic stems. Dendritic growth is simulated based on a Markov process with two hidden parameters: the number of terminal tips to be added, or degree (m), and the path distance from the soma (t). At each bifurcation, the degree is randomly partitioned among the daughters (with the uniform probability). In other words, similarly to the method of processing of basal trees described for pyramidal cells [8], a uniform partition probability rather than the actual "partition table" (Figure 1) is used for all dendrites.

[Figure 1 here]

In order to decide each new internal branch length, the gamma distribution of branching points vs. path distance from the soma is sampled until a number of points corresponding to m are accumulated to the right of the current position. At this time the nearest of them is taken as the next branching point for the current branch, and the rest are discarded. The new internal branch is partitioned into segments by sequential sampling of the segment length distribution. In contrast, in the case of terminal branches ($m = 1$), new segments are sampled and attached to the branch one by one. In order to determine a point of termination, the local probability of termination is sampled after each attachment. With respect to the algorithm developed to model pyramidal cells [8], in the present study termination of all dendrites, regardless of the value of the hidden parameter m, was enforced at a maximum distance from the soma. This feature was introduced based on the analysis of experimental data and allowed better consistency of simulation results. At a shorter path distance from the soma t, the termination probability [8] is given by the formula that best fits the experimental data:

$$P = \frac{1}{2} + \frac{1}{\pi}\arctan\left(\frac{t-\lambda_1}{\lambda_2}\right), \quad (1)$$

where λ_1 also determines the maximum distance from the soma at which all branches (independently of their pre-assigned degree *m*) terminate. Here λ_2 determines the width of the sigmoid transition.

Phase 2 consists of assigning diameters by sampling a gamma distribution, parameters of which are taken as linear functions of the degree *m*, with the coefficients (four real numbers) extracted from the population of real cells. An additional constraint is used that a daughter diameter cannot exceed the parent diameter. Phase 3 consists in embedding the dendrogram into a 3-d space and is performed exactly as described previously [6, 7], where the method of 3D embedding only was applied to real granule cell dendrograms.

The essential new addition introduced in the present work is the sampling of all individual cell parameters prior to phases 1-3. This process is determined by the parameters G extracted from the population of real cells (Table 1) and proceeds as follows. The total degree of the dendritic tree is sampled as a Poisson number with the mean G1. The number of trees is sampled as two plus a Poisson number with the mean G2. The parameters *alpha* and *beta* of the gamma distribution of bifurcations vs. path distance are determined by sampling the product *alpha* · *beta* from a gamma distribution with parameters α = G3, β = G4; and the ratio *beta* / *alpha* is sampled from a gamma distribution with parameters α = G5, β = G6. Parameter λ_1 of (1) is sampled from a gamma distribution with α = G7, β = G8. Parameter λ_2 of (1) is sampled from a gamma distribution with α = G9, β = G10. The initial dendritic diameter is sampled from a gamma distribution with α = G11, β = G12. The Y coordinate of the first node of each dendritic subtree is set to G13. The X and Z coordinates are sampled

from a centered normal distribution with a standard deviation given by G14 and G15, respectively.

[Table 1 here]

3. Simulation Results

Two examples of virtual granule cells are represented in Figure 2 C, D, as compared to the real granule cells (Figure 2, A, B). Note the unequal path length distribution in dendrograms of real cell A, B, which reflects biological variations along the transversal axis of the dentate gyrus [3, 4]. This detail is well captured by the pair of virtual morphologies (Figure 2, C, D).

[Figure 2 here]

The good visual agreement of all essential morphological features between the two pairs of cells is further confirmed by a statistical analysis of several morphometric measurements taken from the two populations (Figure 3). In particular, the following parameters were extracted (numbers correspond to the abscissa in Figure 3; scaling factor, if any, is given in parentheses):

1, 2 topological asymmetry (x100), as defined in [9];

3, 4: number of trees (x100), defined as the number of terminals minus the number of bifurcations;

5, 6: total number of terminals;

7, 8: mean path distance of bifurcation points from the soma (x10);

9, 10: standard deviation of the path distance of bifurcation points from the soma;

11, 12: mean path distance of terminal tips from the soma;

13, 14: standard deviation of the path distance of terminal tips from the soma;

15, 16: total dendritic area (x0.01);

17, 18: dendritic area "center of mass", defined as the weighted mean path distance from the soma;

19 - 24: magnitudes of the eigenvalues corresponding to the first (19, 20), the second (21, 22) and the third (23, 24) principal components of the distribution of dendritic nodes.

All data were calculated for individual cells, and boxes representing the data were plotted for the entire populations (of real and virtual neurons). All of the P-values are well above the standard level of statistical significance 0.05 (Figure 3). In other words, the two populations are consistent with each other with respect to the given measures.

[Figure 3 here]

4. Discussion and Conclusions

In this work we showed that the task of describing the shape of dentate gyrus granule cells computationally can be solved with an elegant hidden-Markov algorithm. The hidden variables of the algorithm include the expected number of terminal tips of a subtree and the path distance from the soma. These variable have a simple, if speculative, biophysical interpretation. We suggest that the variable *m* determining the number of terminations in a subtree can be related to the number of microtubules in the root branch, and that the path distance from the soma *t* can be related to the time of development and to concentrations of proteins associated with dendritic growth and branching.

The model successfully captures all major dendritic morphometrics of rat dentate granule cells, including topological asymmetry, the number of dendritic trees, total degree, the mean

and the standard deviation of the path distance of bifurcation points from the soma, the mean and the standard deviation of the path distance of terminal tips from the soma, the total dendritic area and the dendritic area center of mass, and the eigenvalues corresponding to the principal components of the distribution of dendritic nodes (Figure 3). The total amount of information used by the algorithm (Table 1) is substantially smaller (about one thousand times) than that representing a single digitized neuron.

Parts of the algorithm used here were described in previous works [5-8], where the objects of study were CA3 and CA1 pyramidal cells. In these earlier studies, each virtual cell was generated based on one selected real prototype, taking into account the statistical measures of the rest of the population only to a limited extent. Specifically, a number of cell parameters were simply copied from the corresponding prototype cell. These parameters included the geometry of the initial dendritic segments and the distributions of branching and termination points in the given cell, described by analytical functions.

An essential new element introduced in the present work is an algorithm which samples, from population measures, all cell input parameters that were previously "inherited" from individual prototype cells. Therefore, each simulated virtual cell in the present work is equally related to any one of the given population of real cells, and is not generated by modification of one of them. In addition, the present work expanded the domain of applicability of the model [5, 8], originally developed for pyramidal neurons, to granule cells, thus effectively resulting in the homogeneous algorithmic description of all principal cells of the rat hippocampus.

Acknowledgements

The authors are indebted to Dr. Brenda Claiborne for sharing the neuronal reconstruction digital files and to Dr. Stephen Senft for valuable discussions and feedback on previous versions of the manuscript. This work was supported in part by Human Brain Project Grant R01 NS39600, funded jointly by NINDS, NIMH (National Institutes of Health), and the National Science Foundation.

References

[1] G.A. Ascoli, J.L. Krichmar, S. Nasuto, and S.L. Senft, Generation, description and storage of dendritic morphology data, Phil. Trans. Roy. Soc. B 356 (2001):1131-1145.

[2] G. A. Ascoli, Neuroanatomical algorithms for dendritic modelling, Network 13 (2002):247-260.

[3] N.T. Carnevale, K.Y. Tsai, B.J. Claiborne, and T.H. Brown, Comparative electrotonic analysis of three classes of rat hippocampal neurons, J. Neurophys. 78 (1997): 703-720.

[4] L.L. Rihn and B.J. Claiborne, Dendritic growth and regression in rat dentate granule cells during late postnatal development, Brain Res. Dev. Brain Res. 54 (1990):115-124.

[5] A.V. Samsonovich and G.A. Ascoli, A complete algorithmic description of dendritic morphology in hippocampal pyramidal cells. 2003 Abstract Viewer and Itinerary Planner, Program No. 144.8. (Washington, DC: Society for Neuroscience, CD-ROM, 2003).

[6] A.V. Samsonovich and G.A. Ascoli, Statistical morphological analysis of hippocampal principal neurons indicates cell-specific repulsion of dendrites from their own cell, J. Neurosci. Res. 71 (1993) 173-187.

[7] G.A. Ascoli and A.V. Samsonovich, Bayesian morphometry of hippocampal cells suggests same-cell somatodendritic repulsion, in: T. G. Dietterich, S. Becker, and Z. Ghahramani, Eds., Advances in Neural Information Processing Systems, Vol. 14 (Cambridge, MA: MIT Press, 2003) 133-139.

[8] A.V. Samsonovich and G.A. Ascoli, Statistical determinants of dendritic morphology in hippocampal pyramidal neurons: a hidden Markov model, Hippocampus (in press).

[9] J. Van Pelt, H.B.M. Uylings, R.W.H. Verwer, R.J. Pentney and M.J. Woldenberg, Tree asymmetry - a sensitive and practical measure for binary topological trees. Bull. Math. Biol. 54(1992):759-784.

Tables

Table 1. *Population input parameters of the algorithm.* Units of all dimensional values are μm. The G values were extracted numerically from the population of Claiborne granule cells.

Param.	G1	G2	G3	G4	G5	G6	G7	G8	G9	G10	G11	G12	G13	G14	G15
Value	16.81	0.67	22.5	6.7	2.32	13.09	31.41	12.94	7.0	1.0	18.4	0.16	6.0	2.5	1.0

Legends

Figure 1. *The "partition table" of granule cells.* The diagram represents the distribution of partitions of the number of terminal tips (also called the degree of a subtree) at bifurcation points in the entire population of Claiborne granule cells. Here, as in [8], the likelihoods of partitions are normalized within each column separately, such that their sum is equal to the number of nonempty entries in the column.

Figure 2. *Examples of granule cell dendritic morphologies.* A, B: real granule cells traced from a rat dentate gyrus [2-4]. A: cell 725883B; B: cell 524892B. Left: 3-d shape; right: dendrogram; line thickness represents the dendritic diameter. C, D: virtual dendritic morphologies from the 36 cells computer-generated in the first run of the final version of the algorithm and used in the statistical analysis (Figure 3).

Figure 3. *Statistical comparison of distributions of emergent parameters in real and virtual granule cells.* Parameters and their scaling factors are defined in the text (Section 3: Simulation Results). Odd and even boxes correspond to real and virtual cells, respectively. All dimensional quantities are in microns. Boxes have lines at the lower quartile, median, and upper quartile values. The whiskers show the extent of the rest of the data. Crosses represent outliers with values beyond the ends of the whiskers. Circles in between each pair of boxes represent the P-values (scaled by the factor 1000) of the Wilcoxon rank sum test that two populations are statistically identical with respect to the given parameter. If a circle is missing, the corresponding P-value is above the upper limit of the plot.

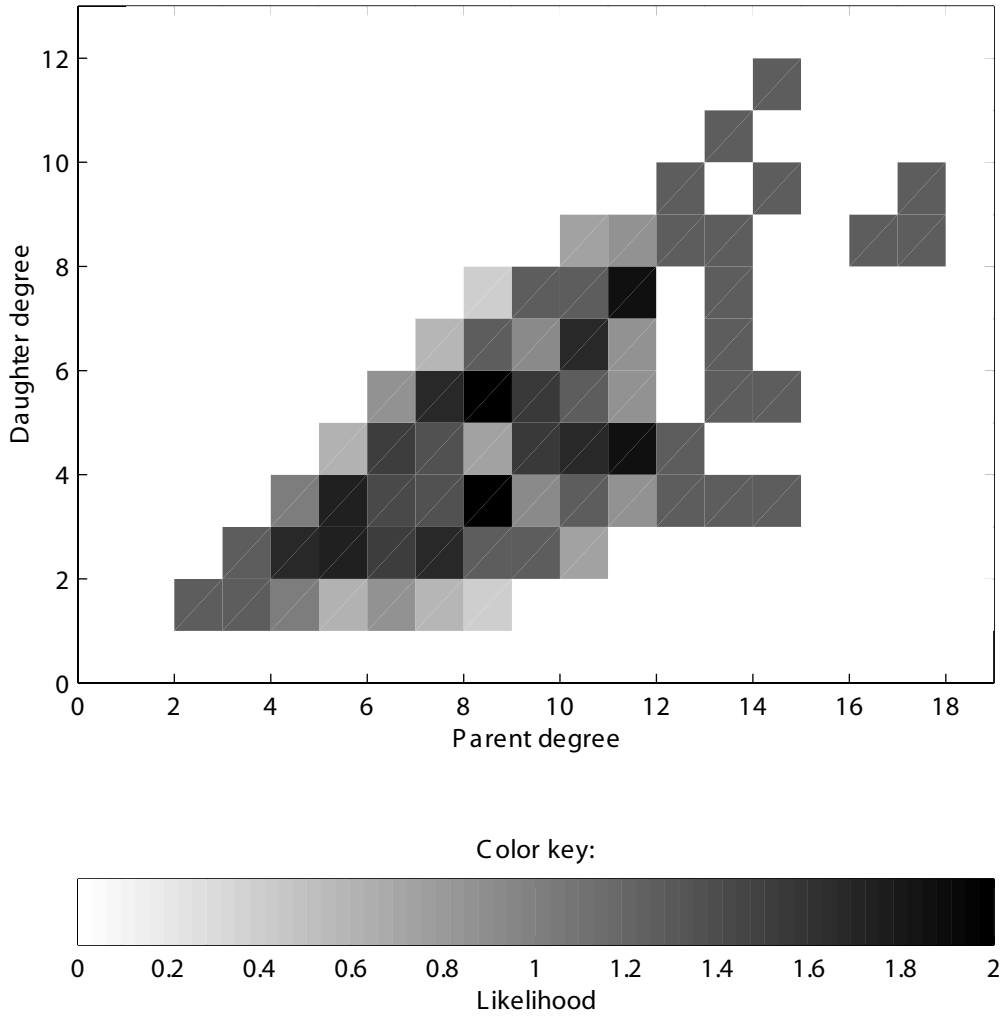
Daughter degree
Parent degree
0
2
4
6
8
10
12
14
16
18

Color key:
0
0.2
0.4
0.6
0.8
1
1.2
1.4
1.6
1.8
2
Likelihood

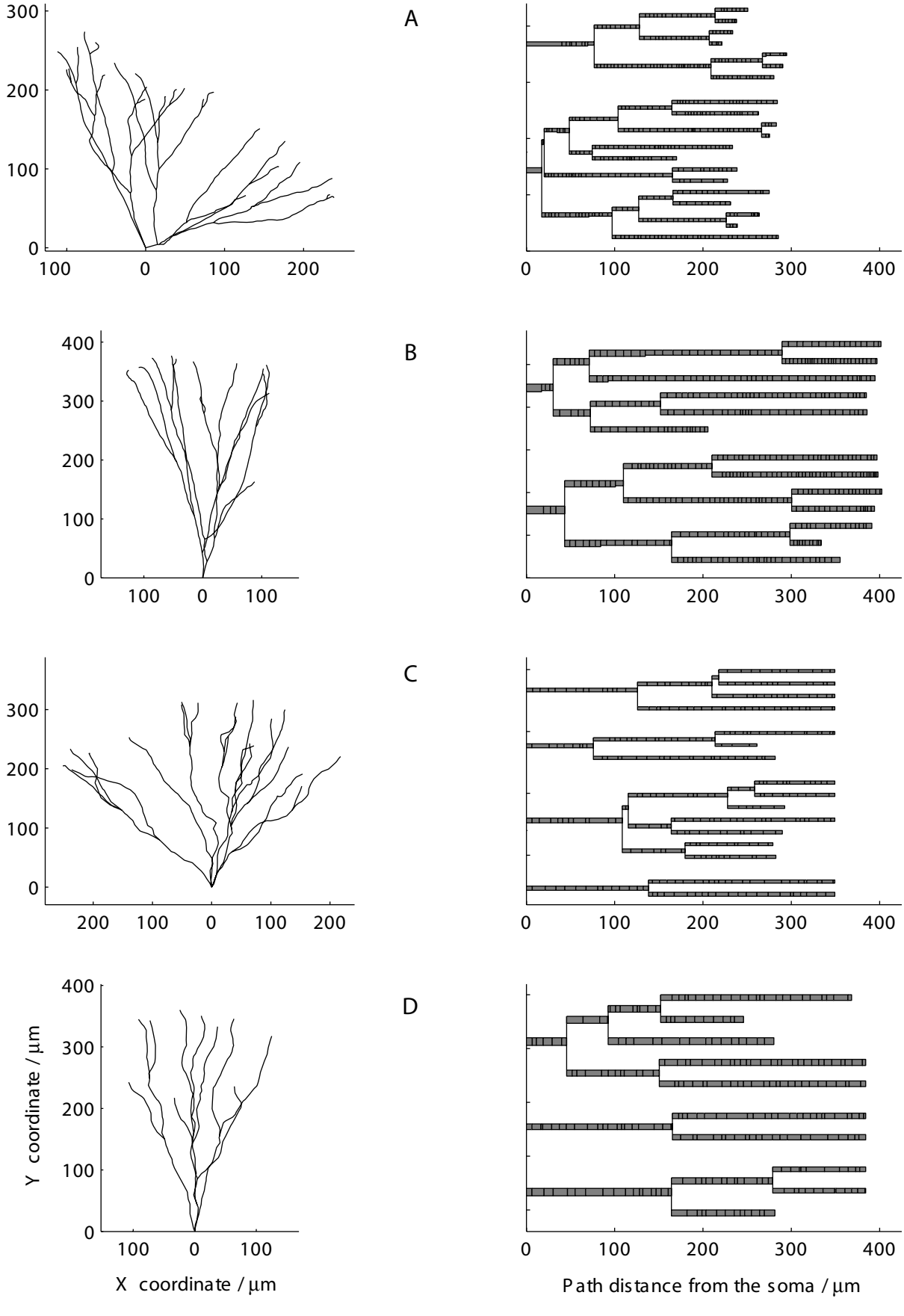
A
B
C
D
Y coordinate / µm
X coordinate / µm
Path distance from the soma / µm

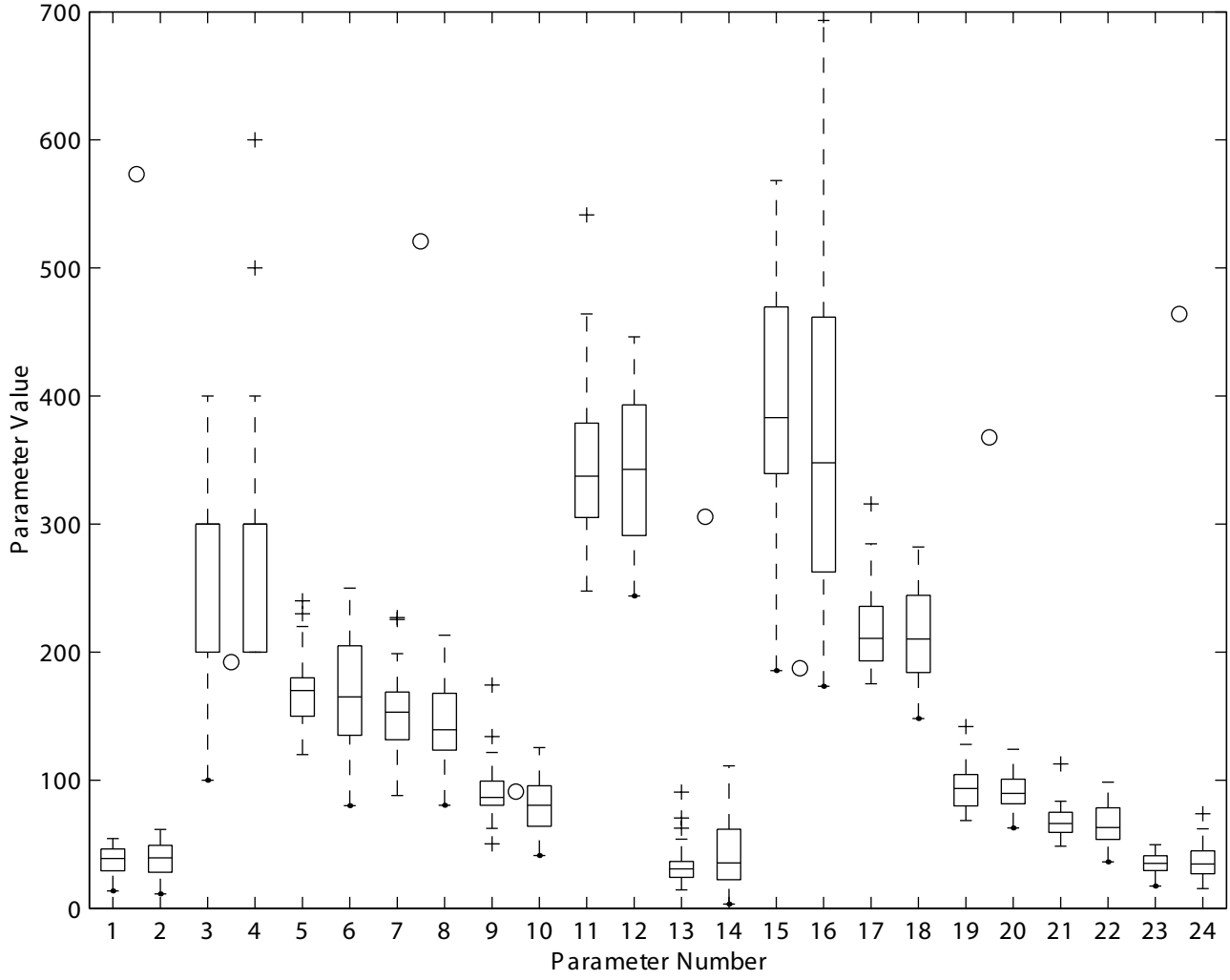
700
600
500
400
300
200
100
0
Parameter Value
1 2 3 4 5 6 7 8 9 10 11 12 13 14 15 16 17 18 19 20 21 22 23 24
Parameter Number